Electron-Phonon Coupling associated transport properties in Alkaline Earth Chalcogenide: A Case Study of CaS

Maitry Joshi, Prafulla K. Jha*

Department of Physics, Faculty of Science, The Maharaja Sayajirao University of Baroda, Vadodara – 390002, Gujarat, India.

Abstract

We present a comprehensive study of the phonon-limited transport properties in alkaline earth chalcogenide CaS, using density functional theory based first-principles calculations integrated with electron-phonon coupling. We calculated thermal and electrical conductivities at room temperature 1.61 W/mk and $26\times10^4\ \Omega^{-1}m^{-1}$, respectively. These properties are sensitive to the electronic band structure dispersion, characterized by the effective mass. Spin-orbit coupling was found to have negligible influence on the carrier transport. Our study highlights the significance of electron-phonon coupling in determining carrier conductivity and scattering mechanisms. We observed that carriers in CaS are confined within a narrow energy range near the band extrema, with electron-phonon scattering dominating over phonon-phonon interactions. These findings suggest opportunities for enhancing carrier dynamics through dimensional confinement and chemical modifications.

1. Introduction

Materials science is pivotal to technological advancements, and the ability to predict material properties before synthesis has become a cornerstone of modern materials research

[1,2]. Semiconductors, among various material classes, are indispensable due to their exceptional adaptability and critical role in optoelectronic and nanoelectronics applications [3-5]. Carrier transport, a key factor in device performance, can be tailored to meet application-specific requirements. The effectiveness of artificial intelligence-based systems is profoundly influenced by the material framework employed, emphasizing the importance of ongoing research and development in this field [6,7]. Globally, researchers have been striving to unravel the intricacies of carrier dynamics within materials, as this understanding underpins advancements in nanoelectronics [8], optoelectronics [9], and spintronics [10]. This underscores the necessity of designing novel materials with exceptional properties, such as rapid on-off switching, optimal carrier recombination rates, and high exciton binding energies [11-13]. These attributes, which are crucial for next-generation device applications, are intrinsically linked to carrier mobility a property governed by electronic band dispersion and the material's mechanical characteristics [14,15].

Density functional theory has become a vital tool for investigating material properties and the mechanisms underlying them [16-18]. Accurate prediction of carrier dynamics requires addressing interactions between energy carriers, particularly electron-phonon coupling [19,20]. Recent advancements in density functional theory have integrated electron-phonon coupling, yielding predictions closely aligned with experimental data [21,22]. This interaction is key to understanding properties such as resistivity [23], conventional superconductivity [24], and thermoelectric performance [25]. It also explains phenomena like the Kohn anomaly, Peierls distortions, spectral line broadening in photoemission and vibrational spectroscopy, and the temperature-dependent band gaps of semiconductors [26-28].

A wide range of chalcogenides has been studied for their carrier transport properties [29,30]. However, research on these materials incorporating electron-phonon coupling remains limited. Group II chalcogenides, including CaS, have garnered attention for their stability and

optoelectronic potential. However, the carrier dynamics of CaS remain largely unexplored. This study seeks to address this gap by investigating the role of electron-phonon coupling in modifying carrier transport properties. We performed density functional theory based first-principles calculations integrated with electron-phonon coupling theories to understand the thermal and electrical transport properties of CaS at room temperature.

2. Methodology

Density functional theory calculations were conducted using the Quantum ESPRESSO [31,32] simulation package within the framework of the projector-augmented wave method. The exchange-correlation energy was described using the generalized gradient approximation (GGA) functional [33] within the framework of Perdew-Burke-Ernzerhof. A Γ-centered 16 × 16 × 16 Monkhorst-Pack k-point grid [34] was employed for structural optimizations, and a kinetic energy cutoff of 90 Ry. All atomic positions were relaxed until the residual force components on each atom were below 0.001 eV/Å. The phonon dispersion curve was calculated using density functional perturbation theory and later on it compare with the EPW approach. The centered 6 × 6 × 6 q-point grid was used for better convergence. Maximally-localized Wannier functions [35] are constructed to represent electronic and phononic states with high precision and computational efficiency. The matrix elements are interpolated on ultra-dense k- and q-point grids using Wannier functions, allowing accurate Brillouin zone integration. The electronic transport properties of semiconductor are calculated by the ab initio Boltzmann transport equation. As the EPW code [36] implements the linear Boltzmann transport equation.

3. Results and Discussion

3.1 Structural Properties

The optimized crystal structures of CaS is depicted in Fig. 1(a). Similar to III-V materials, CaS crystallize in the cubic Rocksalt crystal structure in their bulk phase, which is isotropic and contributes to less complex electronic and phonon band dispersions. The optimized lattice constants of CaS is 5.71 Å, aligning well with reported experimental values and previously reported theoretical values [37].

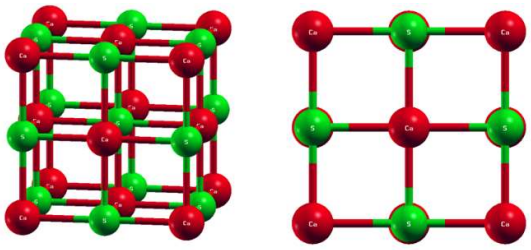

Figure 1 The optimized geometry of unit cell of CaS. The Ca and S atoms are shown in red and green colour, respectively.

Accurate structural optimization signifies reliable inter-atomic force calculations, a prerequisite for predicting ground-state material properties. From the previously reported Bulk modulus, Young's modulus and Poisson's ration, we confirm the mechanical stability of the CaS compound at zero pressure.

3.2 Electronic Properties

In Fig.2 (a), the electronic band structure of CaS in their rocksalt phase is shown along the high symmetry path of the Brillouin zone. Electronic structure calculations reveal that CaS exhibit in-direct bandgaps of 2.02 eV, advantageous for optoelectronic applications and solar cell applications. The direct bandgap supports efficient optical transitions, and the distinct band curvature influences the carrier effective mass, making these materials promising candidates for photocatalytic, photovoltaic, and optoelectronic devices.

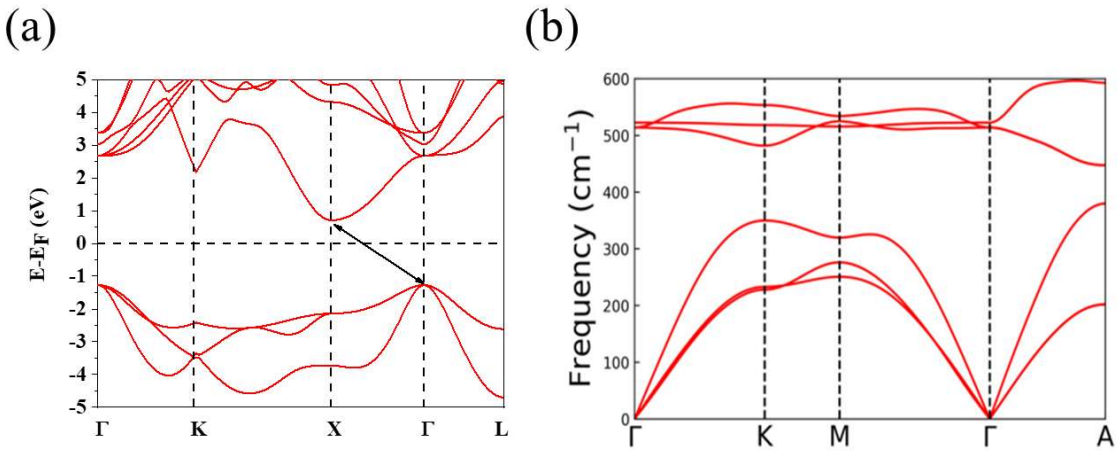

Figure 2 (a) electronic band structure (b) phonon dispersion curve of CaTe at optimized lattice constant value

3.3 Phonon Dispersion and transport properties

We calculate phonon dispersion curves to check dynamical stability of the CaS (as depicted in Fig.2 (b)). Positive frequencies throughout high symmetric path indicates the dynamical stability. The cubic unit cell contains two atoms, yielding six phonon modes: three acoustic (zero frequency at the Γ-point) and three optical, classified as one longitudinal (LO) and two transverse optic (TO) modes. LO-TO splitting, characteristic of non-centrosymmetric crystals, depends on the material's ionicity and polarization. EPW-based dispersion curves show phonon softening due to electron-phonon interactions, which reduce vibrational frequencies through phonon renormalization. Variations in system temperature further enhance anharmonicity, influencing phonon behaviour. E-p interactions can modulate LO-TO splitting, with weaker coupling reducing the gap. We also compare phonon frequency incorporate EPW and without EPW is compared. This clearly suggest that the both are well matched with each other.

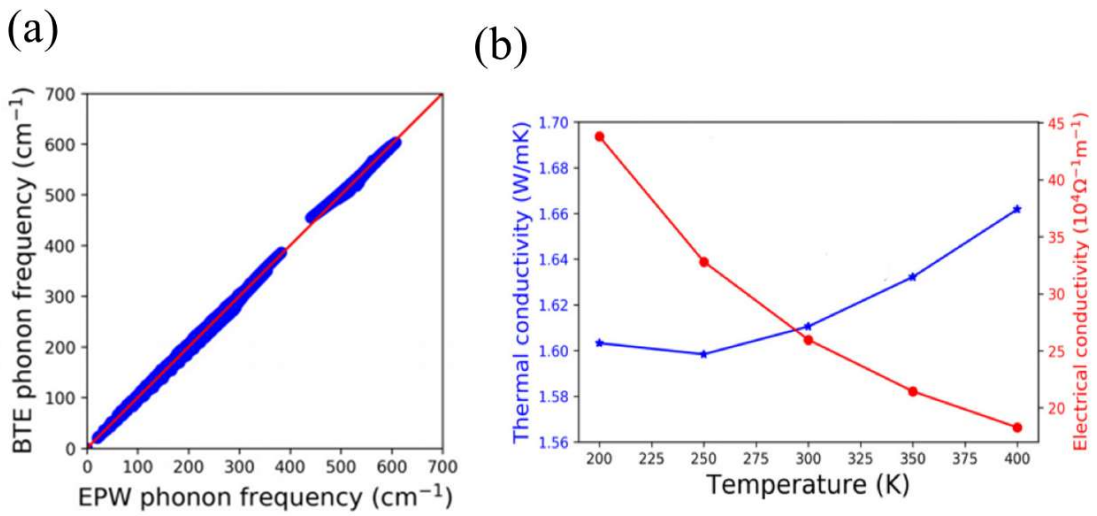

Figure 3 (a) phonon frequency incorporated EPW and without EPW (b) behaviour of thermal conductivity and electrical conductivity with temperature.

We also analyzed Carrier mobility using e-p scattering rates. CaS compound exhibit strong phonon scattering near specific energy levels. We computed thermal conductivity and electrical conductivity as shown in Fig.3 (a,b). At room temperature observed value of thermal conductivity and electrical conductivity is 1.61 W/mk and $26\times10^4\ \Omega^{-1}m^{-1}$, respectively, which is depicted in Fig.3 (b). These values align well with experimental data for similar chalcogenides [38]. The calculated thermal conductivity reflects the strong phonon-phonon scattering, which dominates over electron-phonon interactions at room temperature.

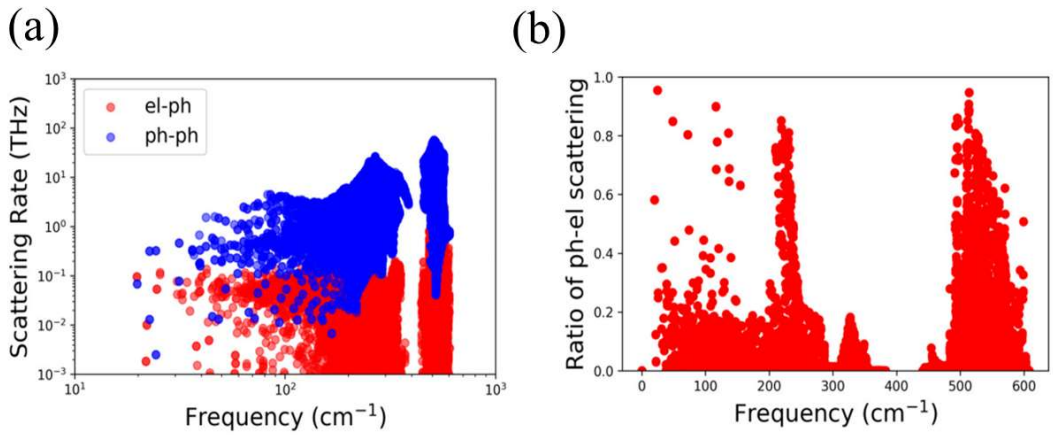

Figure 4 (a) comparison of the electron-phonon scattering rate and phonon-phonon scattering rate (b) the ratio of the electron-phonon scattering and the total scattering rates as a function of phonon frequency.

The carrier mobility was analyzed by calculating e-p scattering rates. Fig.5 (a) illustrates the scattering rates for electrons and holes, showing a significant difference between the two. At room temperature, electron mobility in CaS surpasses hole mobility due to reduced scattering rates near the Fermi level (Fig.5 (b)). This is consistent with observed trends in other semiconductors. Comparisons with materials like GaN and Si underscore the competitive performance of CaS in terms of carrier mobility, highlighting its potential for optoelectronic applications.

4. Conclusions

This study demonstrates the crucial role of electron-phonon coupling in determining the carrier dynamics of CaS. The material exhibits strong phonon-limited transport properties, with thermal and electrical conductivities comparable to those of widely used semiconductors. Carrier mobility calculations reveal distinct scattering mechanisms for electrons and holes, influenced by phonon interactions. Our findings suggest that dimensional confinement or chemical modifications could further enhance carrier mobility, making CaS a promising

candidate for future optoelectronic devices. Future studies could explore the effects of alloying on the transport properties of CaS.

Statement of declaration

No competing/non-competing interest(s) to declare.

Data availability

The data can be made available on reasonable request to the corresponding author.

References

1. Bhattacharya, P., Fornari, R., & Kamimura, H. (2011). *Comprehensive semiconductor science and technology*. Newnes.

2. Song, X., Hu, J., & Zeng, H. (2013). Two-dimensional semiconductors: recent progress and future perspectives. *Journal of Materials Chemistry C*, *1*(17), 2952-2969.

3. Adams, A. R., Silver, M., & Allam, J. (1998). Semiconductor optoelectronic devices. In *Semiconductors and semimetals* (Vol. 55, pp. 301-352). Elsevier.

4. Ghione, G. (2009). *Semiconductor devices for high-speed optoelectronics* (Vol. 116). Cambridge: Cambridge University Press.

5. Singh, J. (2007). *Electronic and optoelectronic properties of semiconductor structures*. Cambridge University Press.

6. Batra, G., Jacobson, Z., Madhav, S., Queirolo, A., & Santhanam, N. (2019). Artificial-intelligence hardware: New opportunities for semiconductor companies. *McKinsey and Company*, *2*.

7. De Luca, C., Lippmann, B., Schober, W., Al-Baddai, S., Pelz, G., Rojko, A., ... & John, R. (2022). AI in Semiconductor Industry. In *Artificial Intelligence for Digitising Industry–Applications* (pp. 105-112). River Publishers.

8. Prasankumar, R. P., Upadhya, P. C., & Taylor, A. J. (2009). Ultrafast carrier dynamics in semiconductor nanowires. *physica status solidi (b)*, *246*(9), 1973-1995.

9. Klimov, V. I. (2000). Optical nonlinearities and ultrafast carrier dynamics in semiconductor nanocrystals. *The Journal of Physical Chemistry B*, *104*(26), 6112-6123.

10. Samarth, N. (2004). An introduction to semiconductor spintronics. In *Solid State Physics* (Vol. 58, pp. 1-72). Academic Press.

11. Rodin, P., & Ivanov, M. (2020). Spatiotemporal modes of fast avalanche switching of high-voltage layered semiconductor structures: From subnano to picosecond range. *Journal of Applied Physics*, *127*(4).

12. Johnston, M. B., & Herz, L. M. (2016). Hybrid perovskites for photovoltaics: charge-carrier recombination, diffusion, and radiative efficiencies. *Accounts of chemical research*, *49*(1), 146-154.

13. Dvorak, M., Wei, S. H., & Wu, Z. (2013). Origin of the variation of exciton binding energy in semiconductors. *Physical review letters*, *110*(1), 016402.

14. Li, S. L., Tsukagoshi, K., Orgiu, E., & Samorì, P. (2016). Charge transport and mobility engineering in two-dimensional transition metal chalcogenide semiconductors. *Chemical Society Reviews*, *45*(1), 118-151.

15. Huang, J., Yuan, Y., Shao, Y., & Yan, Y. (2017). Understanding the physical properties of hybrid perovskites for photovoltaic applications. *Nature Reviews Materials*, *2*(7), 1-19.

16. Orio, M., Pantazis, D. A., & Neese, F. (2009). Density functional theory. *Photosynthesis research*, *102*, 443-453.

17. Bartolotti, L. J., & Flurchick, K. (1996). An introduction to density functional theory. *Reviews in computational chemistry*, 187-216.

18. Engel, E. (2011). *Density functional theory*. Springer-Verlag Berlin.

19. Monserrat, B. (2018). Electron–phonon coupling from finite differences. *Journal of Physics: Condensed Matter*, *30*(8), 083001.

20. Bohnen, K. P., Heid, R., & Renker, B. (2001). Phonon dispersion and electron-phonon coupling in MgB 2 and AlB 2. *Physical review letters*, *86*(25), 5771.

21. Hellsing, B., Eiguren, A., & Chulkov, E. V. (2002). Electron-phonon coupling at metal surfaces. *Journal of Physics: Condensed Matter*, *14*(24), 5959.

22. Heid, R. (2017). Electron-phonon coupling. *Lecture Notes of the Autumn School on Correlated Electrons; Pavarini, E., Koch, E., Scalettar, R., Martin, R., Eds*, 399-427.

23. Park, C. H., Bonini, N., Sohier, T., Samsonidze, G., Kozinsky, B., Calandra, M., ... & Marzari, N. (2014). Electron–phonon interactions and the intrinsic electrical resistivity of graphene. *Nano letters*, *14*(3), 1113-1119.

24. Kulić, M. L. (2000). Interplay of electron–phonon interaction and strong correlations: the possible way to high-temperature superconductivity. *Physics Reports*, *338*(1-2), 1-264.

25. Xu, B., Di Gennaro, M., & Verstraete, M. J. (2020). Thermoelectric properties of elemental metals from first-principles electron-phonon coupling. *Physical Review B*, *102*(15), 155128.

26. Piscanec, S., Lazzeri, M., Mauri, F., Ferrari, A. C., & Robertson, J. (2004). Kohn anomalies and electron-phonon interactions in graphite. *Physical review letters*, *93*(18), 185503.

27. Yam, Y. C., Moeller, M. M., Sawatzky, G. A., & Berciu, M. (2020). Peierls versus Holstein models for describing electron-phonon coupling in perovskites. *Physical Review B*, *102*(23), 235145.

28. Sentef, M. A. (2017). Light-enhanced electron-phonon coupling from nonlinear electron-phonon coupling. *Physical Review B*, *95*(20), 205111.

29. Zhou, J., Liao, B., & Chen, G. (2016). First-principles calculations of thermal, electrical, and thermoelectric transport properties of semiconductors. *Semiconductor Science and Technology*, *31*(4), 043001.

30. Eklöf, D., Fischer, A., Wu, Y., Scheidt, E. W., Scherer, W., & Häussermann, U. (2013). Transport properties of the II–V semiconductor ZnSb. *Journal of Materials Chemistry A*, *1*(4), 1407-1414.

31. Giannozzi, P., Andreussi, O., Brumme, T., Bunau, O., Nardelli, M. B., Calandra, M., ... & Baroni, S. (2017). Advanced capabilities for materials modelling with Quantum ESPRESSO. *Journal of physics: Condensed matter*, *29*(46), 465901.

32. Giannozzi, P., Baroni, S., Bonini, N., Calandra, M., Car, R., Cavazzoni, C., ... & Wentzcovitch, R. M. (2009). QUANTUM ESPRESSO: a modular and open-source software project for quantum simulations of materials. *Journal of physics: Condensed matter*, *21*(39), 395502.

33. Ziesche, P., Kurth, S., & Perdew, J. P. (1998). Density functionals from LDA to GGA. *Computational materials science*, *11*(2), 122-127.

34. Morgan, W. S., Jorgensen, J. J., Hess, B. C., & Hart, G. L. (2018). Efficiency of generalized regular k-point grids. *Computational Materials Science*, *153*, 424-430.

35. Mostofi, A. A., Yates, J. R., Lee, Y. S., Souza, I., Vanderbilt, D., & Marzari, N. (2008). wannier90: A tool for obtaining maximally-localised Wannier functions. *Computer physics communications*, *178*(9), 685-699.

36. Poncé, S., Margine, E. R., Verdi, C., & Giustino, F. (2016). EPW: Electron–phonon coupling, transport and superconducting properties using maximally localized Wannier functions. *Computer Physics Communications*, *209*, 116-133.

37. Labidi, S., Boudjendlia, M., Labidi, M., & Bensalem, R. (2014). First principles calculations of the structural, elastic, and thermal properties of the rocksalt CaX (X= S, Se, Te). *Chinese Journal of Physics*, *52*(3), 1081-1090.

38. Roychowdhury, S., Samanta, M., Perumal, S., & Biswas, K. (2018). Germanium chalcogenide thermoelectrics: electronic structure modulation and low lattice thermal conductivity. *Chemistry of Materials*, *30*(17), 5799-5813.